Preprints of the 19th World Congress
The International Federation of Automatic Control
Cape Town, South Africa. August 24-29, 2014

Adjoint assisted geometry design of a feedback controlled missile ⋆

Kuan Waey Lee * **William H. Moase** * **Andrew Ooi** *
Chris Manzie *

* *Department of Mechanical Engineering, The University of Melbourne, Parkville, Victoria 3010 Australia*
(e-mail: kuanl@student.unimelb.edu.au; moasew@unimelb.edu.au; a.ooi@unimelb.edu.au; manziec@unimelb.edu.au)

Abstract: A novel optimisation framework using an adjoint cost sensitivity calculation, and integrating computer simulations of fluid dynamics, rigid body dynamics and control is proposed. A generic tail-fin steered missile under closed-loop control is used to show that the framework is able to generate a detailed geometrical tail-fin design and tune control performance parameters that are directly related to the range and manoeuvrability of the missile. It is shown that this new methodology is able to reduce the aerodynamic drag by 2% and the tracking error by about 3% relative to the original design.

Keywords: Aerospace; Parametric optimization; Large scale optimization problems.

1. INTRODUCTION

The use of computer simulations as part of the design process is becoming increasingly common in complex and multi-disciplinary engineering products. For missile design, multi-point geometry optimisation ((Anderson et al. (2000)) and trajectory and geometry optimisation (Tekinalp and Bingol (2004) and Yang et al. (2012)) have been reported in the literature. These previous studies utilised low fidelity semi-empirical aerodynamic models such as Missile DATCOM (Vukelich et al. (1988)) rather than modern computational fluid dynamics (CFD) models to generate the aerodynamic data. An obvious criticism of these methods is the accuracy of the semi-empirical aerodynamic models. Moreover, these models implicitly place limitations on both the fidelity and novelty of the shapes that can be generated by the optimiser.

The field of aerodynamic shape optimisation was pioneered by Lighthill (1945) who utilised analytical inverse field methods to determine an optimal shape for a known pressure distribution. More recently, the adjoint method has gained popularity due to the computational efficiency of the method. Jameson (1988) was the first to demonstrate the capability of the adjoint method in calculating the sensitivity of an aerodynamic functional with respect to the geometry design variables with just two simulations. A *primal* simulation is used to capture the behaviour of the physical system and an *adjoint* simulation is used to calculate the gradient of a cost function with respect to all of the design variables. In comparison, calculating the gradient of a cost function using finite differences would require at least $\mathcal{N}+1$ simulations, where $\mathcal{N}$ is the number of design variables. The gradient can then be used within a gradient-based optimiser to find a local minimum. Jameson's work was initially concerned with just optimisation of geometry at a single steady-state, but has since been extended for multi-point optimisation (Reuther et al. (1997)), rotorcraft blade optimisation (Economon et al. (2012)) and aerofoil optimisation with a predefined pitching motion (Economon et al. (2013)). Adjoint methods are limited in that the solution can become entrapped in local minima. The alternative is to use global optimisation methods to overcome this, but global methods require much higher computational resources especially as the number of design variables increases. In Lee et al. (2013), a global extremum seeking method is proposed that utilises semi-converged CFD evaluations to reduce the computational load.

In order to optimise the performance of an aircraft undertaking a set of manoeuvres, one may be tempted to simultaneously compute both the fluid dynamics and the feedback-controlled rigid-body dynamics. Such a task is, however, computationally expensive. Moreover, a complication is introduced by the fact that the achieved aircraft trajectory depends upon the controller, which is typically tuned to the aircraft geometry. In order to address these issues, this paper considers a high velocity regime where the aerodynamic forces acting on the aircraft are adequately described by steady flow. Note that it is common practice in missile modelling to consider only steady flow and to neglect aerodynamic rate effects (see Menon and Ohlmeyer (2001) and Siouris (2004)). A set of CFD simulations is performed in order to map the aerodynamic forces acting on the aircraft for a variety of flow regimes. These maps are then used in a rigid-body dynamic simulation of the aircraft undertaking a set of commanded manoeuvres. An optimiser tunes both the controller gains and the aircraft geometry in order to maximise the aircraft performance, which is expressed in terms of both drag and the ability

⋆ This work was supported by the Australian Research Council's Linkage Projects funding scheme (LP110200025). Support of BAE Systems Australia and the Defence Sciences Institute is also acknowledged.

of the aircraft to track its commanded trajectory. Further to this, cost function gradients are calculated through a novel combination of an adjoint approach for the CFD and a finite-differencing approach for the (computationally cheap) rigid-body dynamics.

2. PROBLEM DESCRIPTION

Consider an aircraft subject to the dynamics,

$$\dot{x} = f\left(x, r(t), X_d, F(\chi(x), X_i)\right), \tag{1}$$

where:

- x is the system state which may, for example, include states related to the rigid-body dynamics of the aircraft, states related to the control surface dynamics, and states used within a feedback controller for motion control.
- $r(t)$ is a reference signal, defined over the time interval $[0, T]$, that describes a "mission" over which the performance of the aircraft is to be evaluated.
- X_d is a vector of "direct" design parameters which may, for example, include vehicle mass, position of centre of gravity, actuator characteristics, controller tuning parameters and geometrical parameters whose effects can be adequately described by available data/models (without undertaking CFD simulations).
- F is a vector of aerodynamic forces and moments that cannot readily be written it terms of a known algebraic or ordinary differential equation. Instead F is to be found by performing a CFD simulation for the steady flow about the aircraft (or a feature thereof).
- X_i is a vector of design parameters related to the geometry of the aircraft. These design parameters are referred to as "indirect" since they only enter the system dynamics via F.
- $\chi(x)$ is the "pose" or configuration of the aircraft with respect to the incident flow. The mapping from x to χ is typically a simple truncation transformation. For example, χ may be described by aircraft states such air speed, the angle of attack, slip angle, roll angle, and control surface deflections. χ cannot contain quantities such as linear accelerations and angular velocities since their effect on aerodynamic forces cannot easily be captured using *steady* CFD simulations. As a result of this, the proposed approach is most applicable to high velocity aircraft where "rate" effects on aerodynamic forces are typically negligible.

The performance of the aircraft for the "mission" can be written as a cost function,

$$J_r := \int_0^T v\left(x, r(t), X_d, F(\chi(x), X_i)\right) \mathrm{d}t. \tag{2}$$

The design objective is to seek the design parameters $X := (X_d, X_i)$ which optimise the aircraft's performance, in other words,

$$\arg\min_X J_r, \tag{3}$$

subject to $(X_d, X_i) \in \mathcal{D}_d \times \mathcal{D}_i$ where $\mathcal{D}_i$ and $\mathcal{D}_d$ are compact sets.

2.1 Discrete approximation for aerodynamic force maps

Consider a given aircraft geometry so that X_i is fixed. F then maps the aerodynamic forces in terms of the aircraft pose. It is reasonable to constrain the pose to a compact set, $\chi \in \mathcal{G}$. Nonetheless, even under these conditions, the domain of F is continuous. Recalling that F can only be "discovered" through CFD simulations, then a single CFD simulation for a given value of χ reveals only one point on the mapping, $F(\cdot, X_i)$. It follows that only a finite number of points on the mapping can be found using CFD simulations, and an interpolation scheme must then be used to approximate F for those values of χ that are not tested. Suppose CFD simulations are performed for n values of χ, denoted by $\chi_1, \ldots, \chi_n$. Then the interpolated mapping $\hat{F}_k(\chi, X_i)$ should have the property that, for any $\epsilon > 0$, there is a n^* such that for all $n > n^*$, $\chi \in \mathcal{G}$ and $X_i \in \mathcal{D}_i$,

$$\left\| \hat{F}_k\left(\chi, X_i\right) - F\left(\chi, X_i,\right) \right\| < \epsilon. \tag{4}$$

3. OPTIMISATION FRAMEWORK

3.1 The Adjoint Method

The adjoint method is a means of calculating the gradient of the cost function with respect to the design variables. The derivation of the adjoint equations following from Nadarajah and Jameson (2000) and Economon et al. (2012) are reproduced here.

Consider a cost function J, that is a function of the flow-field quantities, U, and geometric design variables (indirect design variables) X_i.

$$J = J\left(U, X_i\right). \tag{5}$$

In aerodynamic studies, the cost functions of interest are predominantly some function of the pressure over the surface boundary S of the aircraft. Let the class of these functionals be written as,

$$J = \int_S \boldsymbol{d} \cdot (p \boldsymbol{n_S})\, ds, \tag{6}$$

where, $\boldsymbol{d}$ is a force projection vector, p is the pressure and $\boldsymbol{n_S}$ is the local normal vector on the surface.

By calculus of variations a change in X_i results in a change in the cost,

$$\delta J = \frac{\partial J}{\partial U}\delta U + \frac{\partial J}{\partial X_i}\delta X_i. \tag{7}$$

It is expensive to compute variations in the flow-field quantities, δU, that is, each variation will require an additional CFD simulation. The aim of the adjoint approach is to eliminate this term in (7). Suppose that the governing equations of the flow are introduced in the form of an equality constraint,

$$R\left(U, X_i\right) = 0. \tag{8}$$

For example, $R\left(U, X_i\right)$ could be the conservative form of the compressible Euler equations. The variation in (8) is,

$$\delta R = \left[\frac{\partial R}{\partial U}\right]\delta U + \left[\frac{\partial R}{\partial X_i}\right]\delta X_i = 0. \tag{9}$$

Equation (7) can be combined with (9) via a Lagrange Multiplier, ψ, which gives,

$$\begin{aligned}\delta J &= \frac{\partial J}{\partial U}\delta U + \frac{\partial J}{\partial X_i}\delta X_i - \psi\left(\left[\frac{\partial R}{\partial U}\right]\delta U + \left[\frac{\partial R}{\partial X_i}\right]\delta X_i\right) \\ &= \left\{\frac{\partial J}{\partial U} - \psi\left[\frac{\partial R}{\partial U}\right]\right\}\delta U + \left\{\frac{\partial J}{\partial X_i} - \psi\left[\frac{\partial R}{\partial X_i}\right]\right\}\delta X_i.\end{aligned} \tag{10}$$

Suppose ψ is chosen such that,

$$\left[\frac{\partial R}{\partial U}\right]\psi = \frac{\partial J}{\partial U}. \tag{11}$$

Equation (11) is called the adjoint equation, and with an appropriately defined flow field and boundary conditions, this adjoint PDE can be implemented and solved using the same numerical computer code that is used to solve the governing equations of the flow.

Substituting (11) into (10) eliminates the term δU. The change in the cost functional is,

$$\delta J = G\delta X_i, \tag{12}$$

where the gradient, G, is given by,

$$G = \frac{\partial J}{\partial X_i} - \psi\left[\frac{\partial R}{\partial X_i}\right]. \tag{13}$$

3.2 Modified Adjoint Method

An overview of the optimisation framework is provided in Figure 1. Let X_0 denote the initial set of design variables. The design variables are separated into indirect design parameters, X_i, and direct design parameters, X_d.

For each iteration of the optimiser, the following steps are performed:

(1) The CFD solver is executed for each configuration and this is used to calculate the lift, drag and moment aerodynamic values, $F(\chi_k, X_i)$.
(2) The maps of the aerodynamic forces are then utilised within a simulation of the feedback-controlled rigid-body dynamics for a series of commanded manoeuvres, and a cost function, J_r, is evaluated.
(3) The derivatives of J_r with respect to X_d and $F(\chi_k, X_i)$ are calculated by means of finite differences (requiring multiple executions of step 2).
(4) An adjoint CFD simulation is performed, using knowledge of both the primal CFD states and the derivatives of J_r with respect to $F(\chi_k, X_i)$. The result of the adjoint CFD is the derivative of J_r with respect to X_i.

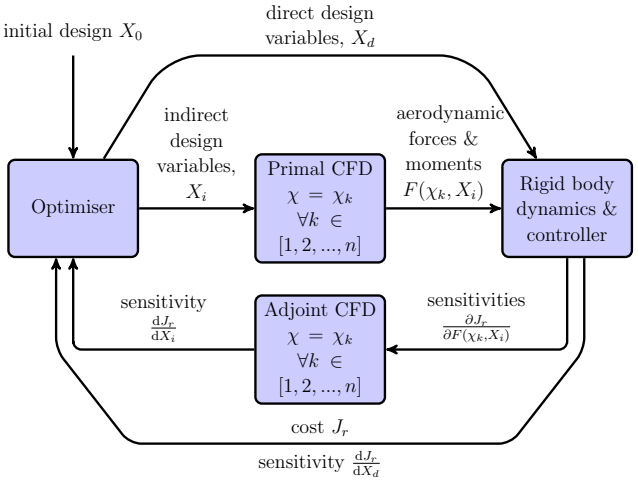

Fig. 1. Optimisation framework

Remark 1. Consider the isolated task of calculating the derivative of J_r with respect to X_d and $F(\chi_k, X_i)$. In this work, the derivative is approximated using finite-difference, which requires many simulations of the feedback-controlled rigid-body dynamics per derivative calculation. This computational cost could be reduced by instead using an adjoint based approach (without making any other change to the proposed framework). The resulting optimisation framework would then have and "inner" adjoint solver for the CFD, and an "outer" adjoint solver for the rigid-body dynamics. However, for the case at hand, the computational effort associated with simulations of the rigid-body dynamics is insignificant compared to that of the CFD. Thus the computational benefits of using an "outer" adjoint solver are small when weighed against the effort required to develop such a solver.

The following describes step 4 in detail. It can be seen that,

$$\frac{\mathrm{d}J_r}{\mathrm{d}X_i} = \sum_k \frac{\partial J_r}{\partial F(\chi_k, X_i)}\frac{\mathrm{d}F(\chi_k, X_i)}{\mathrm{d}X_i}. \tag{14}$$

Suppose that a force projection vector of the form,

$$\boldsymbol{d} = \sum_k \frac{\partial J_r}{\partial F(\chi_k, X_i)}\boldsymbol{H}, \tag{15}$$

is used, where the derivatives of J_r with respect to $F(\chi_k, X_i)$ were found in step 3. In order to calculate the gradient in (14) via the adjoint method, we require each row of $\boldsymbol{H}$ in (15) to correspond to the forces and moments in the vector F.

The derivative of J_r with respect to X_i is calculated using just two CFD simulations (one primal and one adjoint) per configuration per optimiser iteration.

An alternative and perhaps more intuitive formulation is to calculate the gradients $\frac{\mathrm{d}F(\chi_k, X_i)}{\mathrm{d}X_i}$ separately by executing an adjoint CFD simulation for each element in F. However, this particular approach requires $\mathcal{M}+1$ CFD simulations (one primal and $\mathcal{M}$ adjoint) per configuration per optimiser iteration, where $\mathcal{M}$ is the number of elements in F.

4. EXAMPLE

4.1 Missile tail-fin shape optimisation

A tail-fin steered missile moving in the pitching plane is considered. Movement is restricted to the vertical plane and a constant speed relative to the flow is assumed. For a three-dimensional, variable speed model both of these restrictions could be removed, but this would result in additional "poses" of the aircraft, and therefore additional CFD evaluations. The rigid-body dynamics model is then,

$$\begin{aligned}\dot{\alpha} &= -\frac{L}{mV} + q,\\ \dot{q} &= \frac{M_Y}{I_{yy}},\end{aligned} \tag{16}$$

where, the angle of attack α and pitching rate q is written in terms of the instantaneous speed V, missile mass m, second moment of inertia I_{yy}, aerodynamic lift L and moment M_Y. It is assumed that the effects of gravity are neglected. At transonic and supersonic speeds, the gravitational force is small in comparison to the

aerodynamic forces, and, the change in instantaneous speed is also not significant for the manoeuvres considered here.

The normal acceleration can be written as,

$$\eta = \frac{V(q - \dot{\alpha})}{\cos\alpha}. \tag{17}$$

The fin actuators are modelled using a second order linear system,

$$\begin{aligned} \dot{\delta} &= \delta_z \\ \dot{\delta_z} &= \omega_a^2\delta - 2\zeta_a\omega_a\delta_z + \omega_a^2\delta_c, \end{aligned} \tag{18}$$

where, δ_c is the commanded fin deflection, δ is the achieved fin deflection, δ_z is the fin deflection rate, ζ_a is the damping ratio and ω_a is the undamped natural frequency of the actuator.

A variety of feedback control schemes have been adopted in missile control. An overview of some common control algorithms can be found in Jackson (2010). A typical hierarchical control scheme consists of target tracking, guidance, autopilot and servomechanism control. The autopilot is responsible for translating the guidance commands into actuator commands.

In this paper, an acceleration-based control system, commonly known as a "three-loop" autopilot is utilised,

$$\begin{aligned} \delta_c &= -K_R q + W_I x_c \\ \dot{x_c} &= -q + K_A(-\eta + K_{DC}\eta_c) \end{aligned} \tag{19}$$

where, the commanded normal acceleration, η_c, is the input, the fin-deflection is the output, and the missile's achieved pitch rate and acceleration form the feedback signals. A linear technique for tuning the four gains of the controller follow from Zarchan (2012), where an equilibrium operating condition is chosen, along with the desired time constant τ, damping ζ and open-loop crossover frequency. The tuning strategy provides a static mapping from τ, ζ and ω_{cr} to the gains K_{DC}, K_A, W_I and K_R. These control design variables can be thought of as direct design parameters, that is, $X_d = [\tau,\, \zeta,\, \omega_{cr}]$.

For the indirect design parameters, consider the geometry of a generic tail-fin controlled missile found in Sooy and Schmidt (2005). The physical schematic and dimensions of the missile is shown in Figure 2. The missile consists of a tangent-ogive nose, a cylindrical body and four tail-fins arranged in a cruciform. The tail-fins have a leading-edge sweep angle of 33.69° and a wedge profile with a thickness-to-chord ratio of 0.07. In this example, only the tail-fins are optimised with the remaining geometry fixed.

The tail-fins are the control surfaces of the missile. A change in the fins' position, alters the flow field around the missile, this in turn changes the aerodynamic forces and moments and ultimately this affects the rigid-body dynamical states given in (16). For pitch axis motion, it can be seen that the aerodynamic forces and moments depend on the states α and δ. It is then necessary to estimate these forces for the entire α-δ state space of the missile.

The DATCOM computer program (Vukelich et al. (1988)) is able to return aerodynamic data based on semi-empirical models. The program is also capable of calculating the overall forces and moments of the missile, based on a

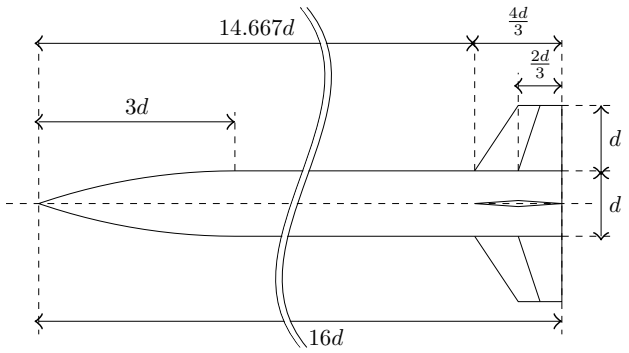

Fig. 2. Schematic of missile nose, body (truncated) and tail

component build-up method, where the aerodynamic data for each individual component (eg. nose, body and fins) are effectively summed up. To alleviate the burden of computing the aerodynamic data for the entire missile, DATCOM is used to generate the aerodynamic data for the nose and body of the missile, and only the tail-fin aerodynamic data at different δ-deflections are generated using steady flow CFD simulations provided by the Stanford University Unstructured (SU^2) package (Palacios et al. (2013)). Therefore the configuration, $\chi = \delta$, and, the vector of the aerodynamic lift, drag and moment of the tail-fin is given by,

$$F := \left[\tilde{D}\ \tilde{L}\ \tilde{M}_Y\right]^\top. \tag{20}$$

DATCOM is used to combine the aerodynamic data of all the various components of the missile together, which gives, $D((\alpha,\delta),X_i)$, $L((\alpha,\delta),X_i)$ and $M_Y((\alpha,\delta),X_i)$. It is these curves which are used in (16).

With F defined as (20), this leads to a matrix,

$$\boldsymbol{H} := \frac{1}{C_\infty}\begin{bmatrix} \cos\delta & \sin\delta & 0 \\ -\sin\delta & \cos\delta & 0 \\ 0 & 0 & \dfrac{-(x-x_0)}{L_{ref}} \end{bmatrix}, \tag{21}$$

which is used in the adjoint CFD simulation, where, $C_\infty = \frac{1}{2}V^2\rho_\infty^2 A_z$. ρ_∞ is freestream density, L_{ref} is the reference length and A_z is the reference area.

The geometry of the tail-fin is deformed using a free-form deformation method (Samareh (2004)), where control points can locally deform the geometry close to where they are specified. 24 control points (or indirect design parameters, X_i) which can only deform the tail-fin in the z-direction are defined. So that the tail-fin remains symmetrical under deformation, each control point at the top of the wing is coupled with the corresponding control point directly below, this means that a positive deformation on the top is mirrored by a negative deformation on the bottom of the tail-fin. The deformations are constrained by maximum and minimum values set in the optimiser. The mesh used to model the tail-fin and the control points are shown in Figure 3.

For a controlled missile, two key performance measures of interest are the manoeuvrability and range. A possible cost function that captures this is,

$$J_r = \int_0^T e(t)^2 dt + w\int_0^T D(t)^2 dt, \tag{22}$$

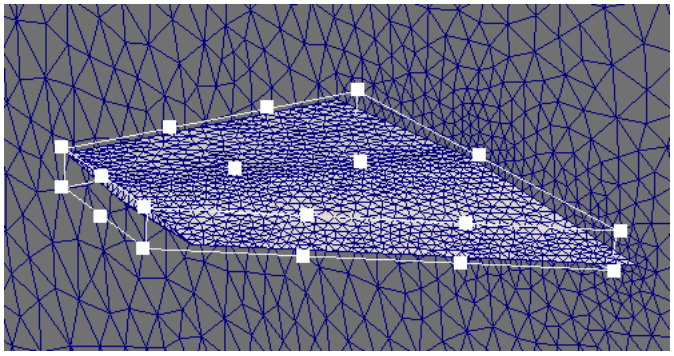

Fig. 3. CFD mesh and geometry deformation control points of tail-fin

where $e(t) = \eta_c - \eta$, is the instantaneous tracking error between the commanded and achieved normal acceleration and $D(t)$ is the instantaneous drag force. A weighting constant w is used to adjust the relative cost of each of component.

4.2 Results

The missile model is subjected to both a positive and negative step change in command acceleration of $5\,\mathrm{ms}^{-2}$ over a 3 second period at a freestream speed of Mach 0.8. An example of the positive step command and response of the missile is shown in Figure 4. The fin deflection rate was recorded to be no more than $100\,\mathrm{rad}\cdot\mathrm{s}^{-1}$ (equivalent to a fin tip rotational speed of $16.67\,\mathrm{ms}^{-1}$). Comparing this value with the freestream Mach speed, it is reasonable to assume that there exists time scale separation between the actuator's speed and the stabilisation of the transonic flow field and therefore justifies the use of steady flow CFD data.

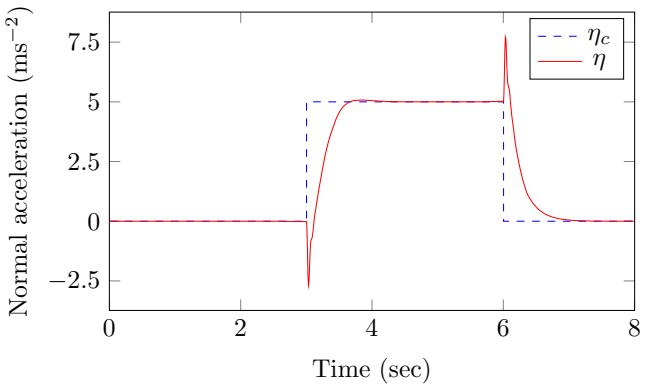

Fig. 4. Step response of missile model

The cost and gradients calculated using the adjoint method are used with an interior point optimisation algorithm (Waltz et al. (2006)) to determine the optimum tail-fin design. Three optimisation test cases are conducted. In Test Case A only the geometry is optimised. In Test Cases B the three control design variables τ, ζ and ω_{cr}, are optimised. In Test Case C both geometry and control parameters are optimised. A cost weighting $w = 3.0 \times 10^{-6}$ is used. The convergence histories for the test cases are shown in Figure 5.

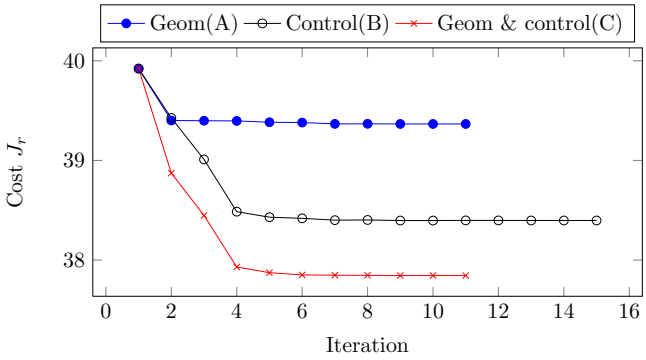

(a) Overall cost

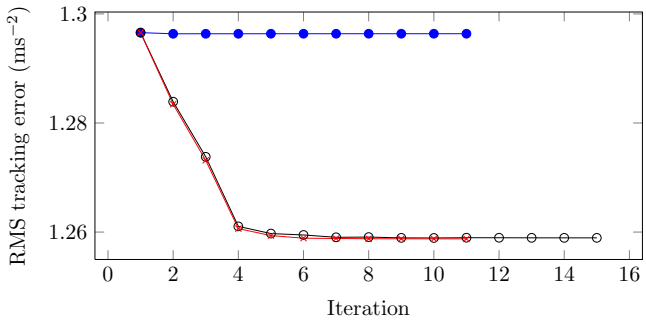

(b) Error component

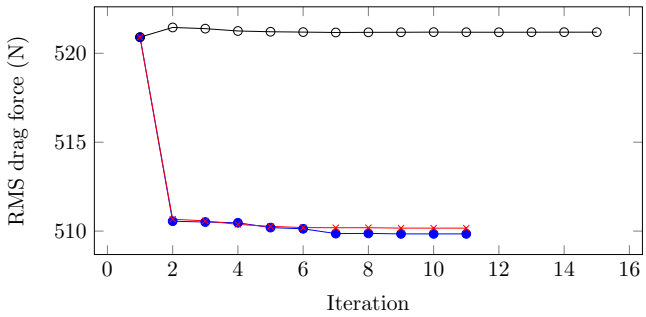

(c) Drag component

Fig. 5. Optimisation convergence history

The result shows that the optimiser was able to converge quite rapidly to the local minimum, requiring only a modest number of function evaluations. In Test Case A the cost was reduced by 1.4%, in Test Case B it is reduced by 3.8%, while in Test Case C the cost was reduced by 5.2%. It is noted that the drag was reduced in both cases A and C by about 2%. While this does not seem to be a significant reduction in absolute terms, it would still be a significant fuel saving. In Test Case A it can be seen that the geometry variables have only a small impact on the tracking error component, and vice versa for Test Case B, the impact of the control parameters on the drag component is small (in fact the drag force is slightly increased). This result indicates that the tracking error depends on the control parameters, and similarly, that the drag force depends on the geometric parameters.

Figure 6 show cut-through sections of the tail-fin at different stations along the span for the initial tail-fin and the two optimised tail-fins. It can be seen that both optimised tail-fins have very similar profiles. The overall height of the tail-fin has been reduced and the fin tapers in

toward its skinniest point at the mid-span. It is interesting to note that the profile of the tip of the fin bulges out again, which emulates the aerodynamic benefits of some traditional wing-tip designs.

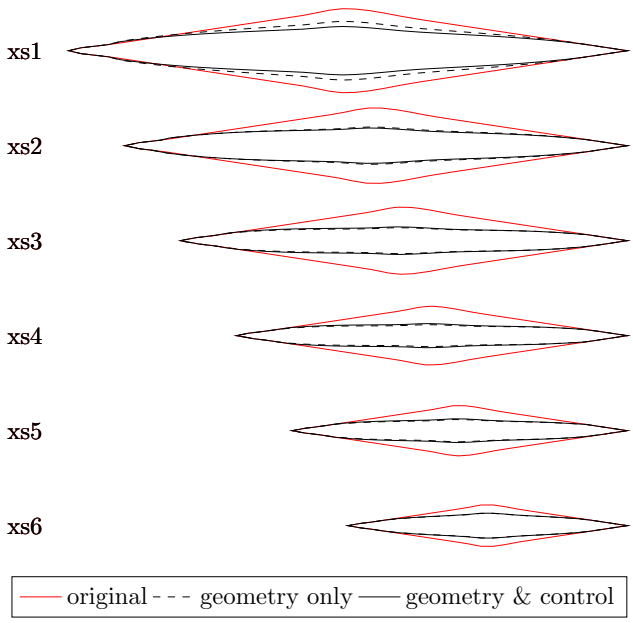

Fig. 6. tail-fin cross-section comparison (vertical scale stretched)

5. CONCLUSION

An optimisation framework integrating an adjoint-based cost sensitivity calculation into an environment consisting of CFD, rigid body dynamics and controller simulation has been developed. This framework, demonstrated through the design of a missile's tail-fin, shows that a locally optimal design can be achieved with only a twofold increase in computational resources and is independent of the number of geometry design variables.

REFERENCES

Anderson, M.B., Burkhalter, J.E., and Jenkins, R.M. (2000). Missile Aerodynamic Shape Optimization Using Genetic Algorithms. *Journal of Spacecraft and Rockets*, 37(5), 663–669.

Economon, T.D., Palacios, F., and Alonso, J.J. (2012). Optimal Shape Design for Open Rotor Blades. In *30th AIAA Applied Aerodynamics Conference*, AIAA-2012-3018. New Orleans, Louisiana.

Economon, T.D., Palacios, F., and Alonso, J.J. (2013). Unsteady Aerodynamic Design on Unstructured Meshes with Sliding Interfaces. In *51st AIAA Aerospace Sciences Meeting including the New Horizons Forum and Aerospace Exposition*, AIAA-2013-0632. Grapevine, Texas.

Jackson, P.B. (2010). Overview of Missile Flight Control Systems. *John Hopkins APL Technical Digest*, 29(1), 9–24.

Jameson, A. (1988). Aerodynamic design via control theory. *Journal of Scientific Computing*, 3(2), 233–259.

Lee, K.W., Moase, W.H., Manzie, C., Hutchins, N., Ooi, A., Vethecan, J., and Riseborough, P. (2013). Is there a need for fully converged CFD solutions? Global extremum seeking applied to aerodynamic shape optimisation. In *3rd Australian Control Conference*. Fremantle, Australia.

Lighthill, M.J. (1945). A new method of two-dimensional aerodynamic design. In *R & M 1111, Aeronatuical Research Council*.

Menon, P.K. and Ohlmeyer, E.J. (2001). Integrated design of agile missile guidance and autopilot systems. *IFAC - Control Engineering Practice*, 9(10), 1095–1106.

Nadarajah, S.K. and Jameson, A. (2000). A Comparison of the Continuous and Discrete Adjoint Approach to Automatic Aerodynamic Optimization. In *38th AIAA Aerospace and Sciences Meeting and Exhibit*, AIAA-2000-0667. Reno, Nevada.

Palacios, F., Alonso, J.J., Duraisamy, K., Colonno, M.R., Aranake, A.C., Campos, A., Copeland, S.R., Economon, T.D., Lonkar, A.K., Lukaczyk, T.W., and Taylor, T.W.R. (2013). Stanford University Unstructured (SU^2): An open source integrated computational environment for multiphysics simulation and design. In *51st AIAA Aerospace Sciences Meeting and Exhibit*. Grapevine, Texas, USA.

Reuther, J., Jameson, A., Alonso, J.J., Rimlinger, M.J., and Saunders, D. (1997). Constrained Multipoint Aerodynamic Shape Optimization Using an Adjoint Formulation and Parallel Computers. *Journal of Aircraft*, 36(1), 51–60.

Samareh, J.A. (2004). Aerodynamic Shape Optimization Based on Free-form Deformation. In *10th AIAA/ISSMO Multidisciplinary Analysis and Optimization Conference*, AIAA-2004-4630. Albany, New York.

Siouris, G.M. (2004). *Missile guidance and control systems*. Springer-Verlag, New York.

Sooy, T.J. and Schmidt, R.Z. (2005). Aerodynamic Predictions, Comparisons, and Validations using Missile DATCOM (97) and Aeroprediction 98 (AP98). *Journal of Spacecraft and Rockets*, 42(2), 257–265.

Tekinalp, O. and Bingol, M. (2004). Simulated Annealing for Missile Optimization: Developing Method and Formulation Techniques. *Journal of Guidance, Control, and Dynamics*, 27(4), 616–626.

Vukelich, S.R., Stoy, S.L., Burns, K.A., Castillo, J.A., and Moore, M.E. (1988). Missile DATCOM Volume I - Final Report. Technical Report AFWAL-TR-86-3091, McDonnell Douglas Missile Systems Company, St. Louis, Missouri.

Waltz, R.A., Morales, J.L., Nocedal, J., and Orban, D. (2006). An interior algorithm for nonlinear optimization that combines line search and trust region steps. *Mathematical Programming*, 107(3), 391–408.

Yang, Y.R., Jung, S.K., Cho, T.H., and Myong, R.S. (2012). Aerodynamic Shape Optimization System of a Canard-Controlled Missile Using Trajectory-Dependent Aerodynamic Coefficients. *Journal of Spacecraft and Rockets*, 49(2), 243–249.

Zarchan, P. (2012). *Tactical and Strategic Missile Guidance*, volume 239 of *Progress in Astronautics and Aeronautics*. AIAA, Reston, Virginia, 6th edition.